Microchimica Acta (2021) 188: 87
https://doi.org/10.1007/s00604-021-04745-w

ORIGINAL PAPER

Sensitive colorimetric aptasensor based on g-C_3N_4@Cu_2O composites for detection of *Salmonella typhimurium* in food and water

Afrooz Tarokh[1] · Azam Bagheri Pebdeni[1] · Hazha Omar Othman[2] · Foad Salehnia[3] · Morteza Hosseini[1,4]

Received: 2 October 2020 / Accepted: 3 February 2021 / Published online: 16 February 2021

Abstract

A new colorimetric aptasensor equipped with a novel composite of graphitic carbon nitride (g-C_3N_4) nanosheets and copper oxide(I) (Cu_2O) nanocrystals is presented for *Salmonella typhimurium* (*S .typhimurium*). The dual-purpose structure of this composite simultaneously contributes to superb peroxidase-like activity and interaction with a label-free aptamer. Although g-C_3N_4@Cu_2O effectively creates a visible blue color following the oxidation of 3,3′,5,5′-tetramethylbenzidine (TMB) in presence of hydrogen peroxide (H_2O_2), this catalytic activity of the composite severely decreases after the interaction with aptamers. In the presence of *S. typhimurium* in sample, aptamers bound to their specific target. Subsequently, g-C_3N_4@Cu_2O catalytic activity was enhanced in proportion to *S. typhimurium* concentration. Under optimized conditions, this aptasensor exhibited an excellent detection performance in a range from 1.5×10^1 to 1.5×10^5 CFU/ml, with a detection limit of 15 CFU/ml. Besides, portable detection of *S. typhimurium* by paper-based model of this method operated successfully in just 6 min. Analysis of spiked milk samples revealed high potential of this method as a sensitive, rapid, and label-free promising tool for *S. typhimurium* detection.

Keywords Colorimetric aptasensor · G-C_3N_4@Cu_2O composite · Peroxidase-like activity · *Salmonella typhimurium* · Foodborne pathogen

Introduction

Every year millions of people become sick or even die because of foodborne diseases [1]. *Salmonella* bacteria as the major cause of foodborne diseases in many countries for at least more than 100 years is a life-threatening problem for millions of people and societies [2]. One of the most medically important *Salmonella* spp. is *S. typhimurium*, a gram-negative bacterium that causes a type of gastroenteritis called salmonellosis [3]. In addition to clinical disorders such as fever, abdominal pain, vomiting, and diarrhea [4], the spread of *Salmonella* to bloodstream may cause pneumonia, meningitis, osteomyelitis, and other devastating diseases. Environmental stress tolerance, widespread distribution, and multiple drug resistance have made this bacterium a serious persistent burden to public health, while no specific treatment is available for it [5, 6].

Common bacterial detection methods are not efficient enough for in situ detection of such an important pathogen. Culture-based methods are so time consuming and laborious, often requiring several days to complete. Furthermore, they need an equipped laboratory with expensive equipment and trained lab personnel [7]. Immunoassay methods depending on antibody-antigen interactions need shorter assay time, but they are not capable enough to detect a pathogen in real time without affecting by interferences [8]. The methods based on polymerase chain reaction (PCR) have high precision and selectivity, but they encounter another problem correlated with sample matrix that could normally contain PCR inhibitors, which can be found in food samples. Moreover, there are difficulties for detecting low number of bacteria in a relatively large amount of sample [7]. Hence, there is need for a sensitive,

✉ Morteza Hosseini
smhosseini@khayam.ut.ac.ir

1 Department of Life Science Engineering, Faculty of New Sciences & Technologies, University of Tehran, Tehran, Iran

2 Department of Chemistry, College of Science, Salahaddin University-Erbil, Erbil, Iraq

3 Center of Excellence in Electrochemistry, Faculty of Chemistry, University of Tehran, Tehran 1417614418, Iran

4 Department of Pharmaceutical Biomaterials, Medical Biomaterials Research Center, Faculty of Pharmacy, Tehran University of Medical Sciences, Tehran, Iran

rapid, and affordable approach. Rapid response time, simple use, lower cost, portability, and free of pre-enrichment step are excellent properties of biosensors for diagnostic purposes [9].

The prominent advantages of colorimetric biosensors (such as high sensitivity, facility, and easiness of signal read out) made them popular in analytical applications [10, 11]. Colorimetric methods have been widely applied in detection of pathogens due to unique properties like showing the results as visible color and fast data record [12, 13]. One of the most common strategies in colorimetric assay is based on the enzymatic conversion of a chromogenic substrate like TMB that can make colorful products in presence of H_2O_2 [14–17].

Aptamers are short synthetic DNA or RNA sequences, which can be designed to detect specific targets such as proteins, ions, bacteria, viruses, and small molecules [18, 19]. In comparison with antibodies, aptamers show more advantages including low cost, great stability, and ease of chemical synthesis [18, 20]. G-C_3N_4 nanosheet has unique features that

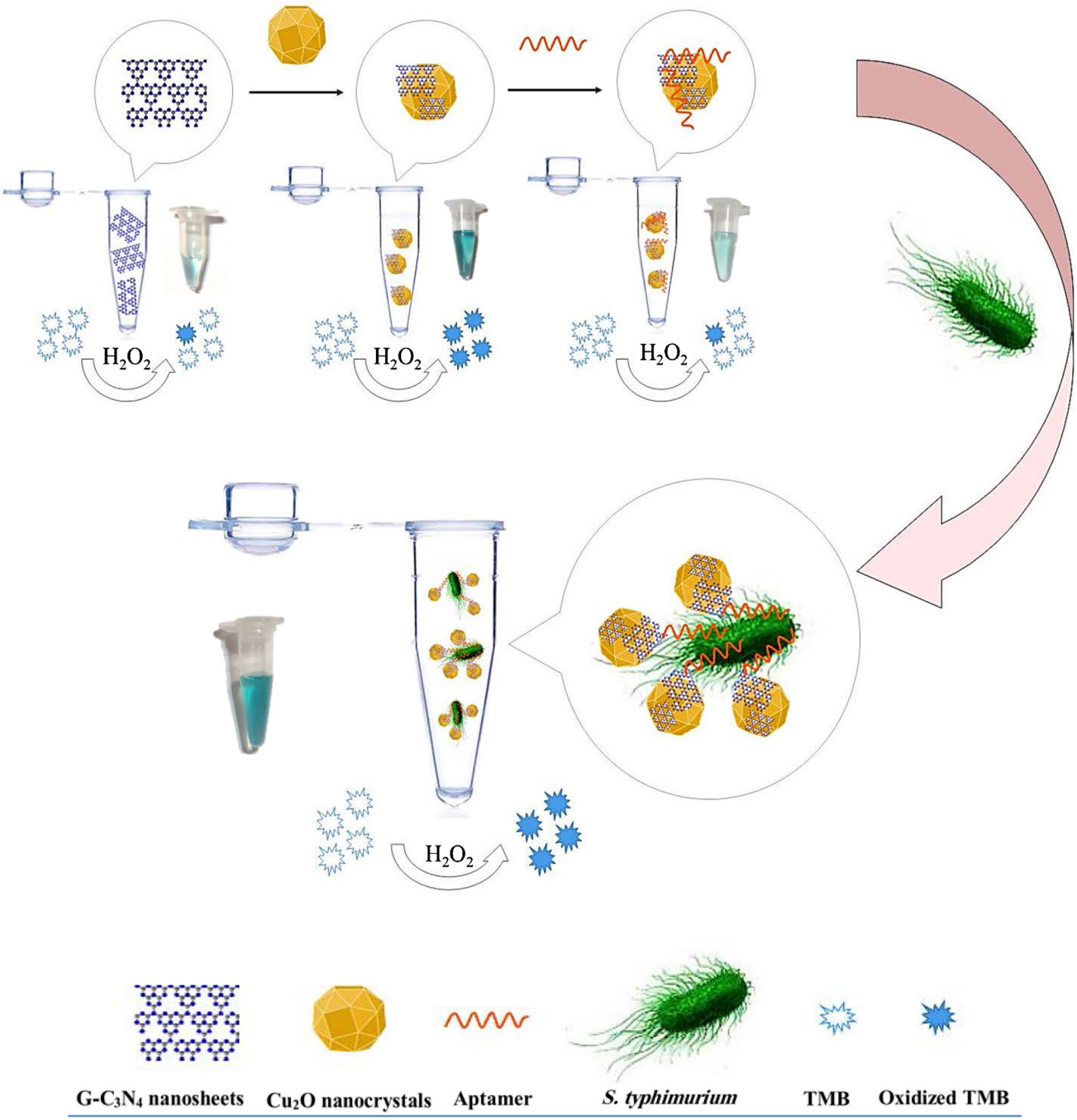

Scheme 1 Schematic illustration of colorimetric aptasensor for *S. typhimurium* detection

have resulted to find application in sensors, drug delivery technologies, and imaging systems [21]. G-C_3N_4 is a metal-free polymeric semiconductor that has attracted significant attention in optics due to the excellent stability, low toxicity, great fluorescence, and biocompatibility [22, 23]. The remarkable peroxidase-like activity of some nanostructures has opened new windows in colorimetric studies [24]. Among them, Cu_2O nanostructures have been used in sensors because of their large surface area and superb catalytic activity [25].

As a point-of-use technology, paper-based analytical devices (PADs) are portable, disposable, and low cost. PADs coupled with colorimetric method can provide semiquantitative results without requiring complicated equipment. Besides, quantitative analysis can be done using common optical technologies such as digital cameras and office scanners joined with image processing software [26, 27].

In this study, a novel composite of g-C_3N_4 and Cu_2O was proposed to design an efficient aptasensor for *S. typhimurium* (Scheme 1). As a colorimetric detection, the peroxidase-like activity of composite was monitored in each step by recording the absorbance after adding TMB and H_2O_2. High peroxidase-like activity of g-C_3N_4@Cu_2O was severely decreased after the interaction with specific aptamers of *S. typhimurium*. Following the addition of *S. typhimurium*, aptamers were attached to the target with high tendency and the peroxidase-like activity of composite was increased in the way that a range of blue colors was achieved. Each obtained blue color was correlated to a certain concentration of *S. typhimurium*, which could be interpreted to quantitative amounts. In order to confirm the practical concentration of bacteria in contaminated samples, the plate count method was applied as a proven method for bacteria counting in microbiology, since the culture-based methods are still the gold standard for detection of *Salmonella* [19, 28]. Finally, paper-based model of this assay was proposed for portable detection of *S. typhimurium* in water and food samples.

Materials and methods

Materials and reagents

Melamine and HNO_3 (for synthesizing g-C_3N_4 nanosheets), $CuSO_4$, KOH and ascorbic acid (for synthesizing the g-C_3N_4@Cu_2O composite), TMB and H_2O_2 (for testing peroxidase-like activity), and Tris-EDTA and HCl (for preparing TE buffer) were all obtained from Merck Millipore Company. Specific aptamer for capturing *S. typhimurium* (5′-TAT GGC GGC GTC ACC CGA CGG GGA CTT GAC ATT ATG ACA G -3′) which has been introduced through research by Joshi et al. [29] was purchased from Nedayefan Company (Tehran, Iran). Lyophilized bacterial strains and bacterial culture media were supplied by Baharafshan Institute of Research and Development (Tehran, Iran). Raw cow milk was obtained from a local market (Tehran, Iran). At all stages, sterile deionized water was applied for preparing solutions and bacterial dilution.

Apparatus

Ultraviolet-visible (UV-Vis) absorption spectra were measured in the range of 200–800 nm using Perkin-Elmer lambda 25 UV-Vis spectrometer. TEM analysis was obtained using a transmission electron microscope (Zeiss, EM10C, 80 KV and Germany) for analyzing the size of g-C_3N_4 nanosheet and the structure of g-C_3N_4@Cu_2O composite. Field-emission scanning electron microscopic (FE-SEM) analysis was accomplished by a XL30 ESEM FEG scanning electron microscope. Dynamic light scattering (DLS) measurements were conducted by a Zetasizer Nano-ZS90 Malvern at room temperature. FT-IR spectroscopy analysis was carried out utilizing a Spectrum Two Fourier-transform infrared Perkin Elmer spectrometer in the range of 4000 to 400 cm^{-1}, at room temperature. Energy dispersive X-ray spectroscopy (EDX) was performed by a Tescan model energy dispersive spectrometer.

Synthesis of g-C_3N_4 nanosheets

G-C_3N_4 nanosheets were synthesized according to previous works [22]. First, 5 g melamine situated in an alumina crucible with a cover was heated at 550 °C for 5 h to make bulk C_3N_4. Then 1 g of prepared bulk C_3N_4 powder was poured to 100 ml of 5 M HNO_3 and then refluxed at 125 °C for 12 h. The product of process was cooled to room temperature, and then centrifuged at 10,000 rpm for 30 min and washed several times with deionized water for neutralization. Afterward, the collected supernatant was exposed to ultrasonic noise for 10 h. Subsequently, the isolated solution of g-C_3N_4 nanosheets was obtained by filtering the supernatant through a 45-μm water phase membrane filter. The concentration of final g-C_3N_4 nanosheets was 300 μg ml^{-1}.

Fabrication of g-C_3N_4@Cu_2O composites

In order to synthesize g-C_3N_4@Cu_2O, first a solution of the prepared g-C_3N_4 nanosheets was exposed to ultrasonic waves for 1 h. Then 0.5 ml of sonicated g-C_3N_4 nanosheets was added into a mixture containing 160 mg of copper(II) sulfate ($CuSO_4$) and 55 ml of deionized water. The entire mixture was poured into a three-neck round-bottom flask and situated under constant magnetic stirring and heating in a water bath. When the temperature of mixture reached to 68 °C, stirring was continued for another 10 min. After that, 20 ml of typical 10% KOH solution was added and the color of solution immediately changed to sky blue and then dark blue. Ten milli-

liters of 0.8 mM ascorbic acid was added to this blue solution and mixed on a magnetic stirrer for 10 min. When the color of solution changed to orange, stirring was continued at 68 °C for another 10 min. After the product of process was cooled to room temperature, the excess residues were separated by centrifugation at 8000 rpm for 1 min and five times washes. The final product was dried at 25 °C and stored in a refrigerator at 4 °C for later use.

Peroxidase-like activity of g-C_3N_4@Cu_2O

TMB was selected as the substrate for checking the peroxidase-like activity of g-C_3N_4@Cu_2O. For this evaluation, different concentrations of TMB (10 μL, 5–8–10–12 and 15 mM) and different concentrations of H_2O_2 (10 μL, 0.5–1–2–3 and 4 M) were both added to 100 μl of g-C_3N_4@Cu_2O for 6 min (as the fixed time obtained for changing the color of composite) and instantly the UV-Vis absorption spectra were measured at constant time intervals. At all stages, a constant standard quartz cell was used for recording the absorption spectra.

Preparation of bacterial culture and serial dilution

Each of the desired bacteria, including *S. typhimurium* (ATCC 14028) (as the target bacterium), *Escherichia coli* (ATCC 35218), *Staphylococcus aureus* (ATCC 29213), and *Pseudomonas aeruginosa* (ATCC 10145), was cultured .In order to prepare cultures from lyophilized bacteria, Brain heart infusion (B.H.I) culture medium was first used. Under sterile conditions, 2 ml of B.H.I liquid medium was added to each vial of lyophilized bacteria by sterile syringe and mixed by shaking gently. Afterwards, two drops of each bacterial suspension were transferred to a plate containing nutrient agar (NA) medium and situated in an incubator at 37 °C for 24 h. Subsequently, another culture was provided by streak plate method from the initial culture in order to prepare separate pure colonies. For each bacterial strain, appropriate amounts of pure colonies were diluted in deionized water in a way that optical density for all four strains at 600 nm (OD_{600}) reached an equal value [9]. The number of bacterial cells related to each stock was estimated by the plate count method as the standard method. Accordingly, a serial dilution of each strain was prepared to provide other concentrations of bacteria.

Colorimetric method for *S. typhimurium* detection

The peroxidase-like activity of g-C_3N_4@Cu_2O was evaluated in different conditions to achieve the best results. First, the concentrations of TMB and H_2O_2 were optimized separately. For aptamer preparation, 1 μl of 100 μM aptamer (solved in TE buffer) was diluted in 19 μl of distilled water and incubated at 95 °C for 5 min. Then, 60 μl of the prepared aptamer was mixed with 40 μl of g-C_3N_4@Cu_2O for each bacterial concentration at different incubation times until the aptamers successfully attached to g-C_3N_4@Cu_2O. For monitoring of this attachment, the peroxidase-like activity of g-C_3N_4@Cu_2O/aptamer was evaluated and recorded regularly. After that, different concentrations of *S. typhimurium* (1.5–1.5 × 10^5 CFU/ml) were added to the same amounts of prepared aptasensor. For detection step, peroxidase-like activity was determined with UV-Vis spectrometer after incubation at room temperature.

Preparation and test of real sample

Milk is one of the most important food that should be evaluated in terms of *Salmonella* absence before consumption. Hence, it was chosen as the real sample for checking the analytical reliability of this aptasensor. For this purpose, at first milk was diluted with deionized water and then, it was centrifuged to obtain the supernatant. Afterwards, this diluted milk was deliberately spiked with known concentrations of *S. typhimurium* (1.5–1.5 × 10^5 CFU/ml). Finally, the spiked milk samples were added to aptasensor (g-C_3N_4@Cu_2O/aptamer) under identical conditions and incubated for 90 min (optimal time for incubation). In order to view results, peroxidase-like activity of each sample was finally evaluated by adding TMB and H_2O_2.

Paper-based model of aptasensor

In order to prepare the appropriate paper, the Whatman filter paper Grade1 was first cut by a CO_2 laser engraver. Then, the PVC sheet was stuck in the back of each paper to barricade permeating of reagents from the bottom of papers. For paper-based analysis, first 3 μl of aptasensor solution was poured on paper-chip deposition zone and after drying, another 3 μl of aptasensor solution was added on paper to improve physical stabilization [30]. Then, 3 μl of a sample containing *S. typhimurium* with certain concentration was dropped on a paper-chip and after drying, another 3 μl of the sample was added. As control, the same volume of a sample without *S. typhimurium* was added to another paper-chip in the same way. After drying, 3 μl of TMB and 3 μl of H_2O_2 were added twice to both of paper-chips, respectively. Although color changes were traced with naked eye, the ImageJ processing program was also used to assess the intensity of blue color.

Results and discussion

Choice of materials

G-C_3N_4 nanosheet as the most stable allotrope of carbon nitride is a chemical and thermal stable analogue of graphite that

has different properties with graphene despite their structural similarities. Compared to the other graphene derivatives, g-C_3N_4 nanosheet has represented more desire to adsorb single-stranded DNA [22]. Thus, aptamers could be adsorbed on the surface of it through π-interactions, in accordance with the purpose of this study. Although g-C_3N_4 nanosheet could accomplish peroxidase-like catalysis of hydrogen peroxide lonely [22], but a material with much stronger peroxidase-like activity was required in order to detect very low concentrations of a microscale bacterium. Cu_2O nanocrystal as a metal oxide nanostructure has demonstrated outstanding peroxidase-like activity for bioanalytical applications [31]. Hence, based on the advantages of g-C_3N_4 nanosheet and Cu_2O nanocrystal, a novel composite of these two nanostructures was synthesized in which the required peroxidase-like activity and the possibility of interaction with aptamer were provided. In order to form a univalent composite, the synthesis steps of Cu_2O nanocrystal and the final composite were combined simultaneously.

Characterization of g-C_3N_4 nanosheets and g-C_3N_4@Cu_2O

For characterization of the structures and verification of correct formation of g-C_3N_4@Cu_2O, the synthesized structures were studied subjecting several analyses, including transmission electron microscopy (TEM), scanning electron microscopy (SEM), UV-Vis spectroscopy, fluorescence spectroscopy, X-ray diffraction (XRD), energy dispersive X-ray analysis (EDX), and EDX mapping analysis. According to TEM image, an average size of 110_130 nm was estimated for g-C_3N_4 nanosheets. Furthermore, TEM image of these nanosheets verified their sheet-like structures (Fig. 1a). The formation of g-C_3N_4@Cu_2O composites was obviously demonstrated by SEM images (Fig. 1b). As shown in Fig. 1b, g, C_3N_4 nanosheets were well mounted on the Cu_2O nanocrystals. As Fig. 1c illustrated, the XRD pattern of g-C_3N_4@Cu_2O was also obtained to provide further evidence of both nanostructures in the composite. The observed peak at

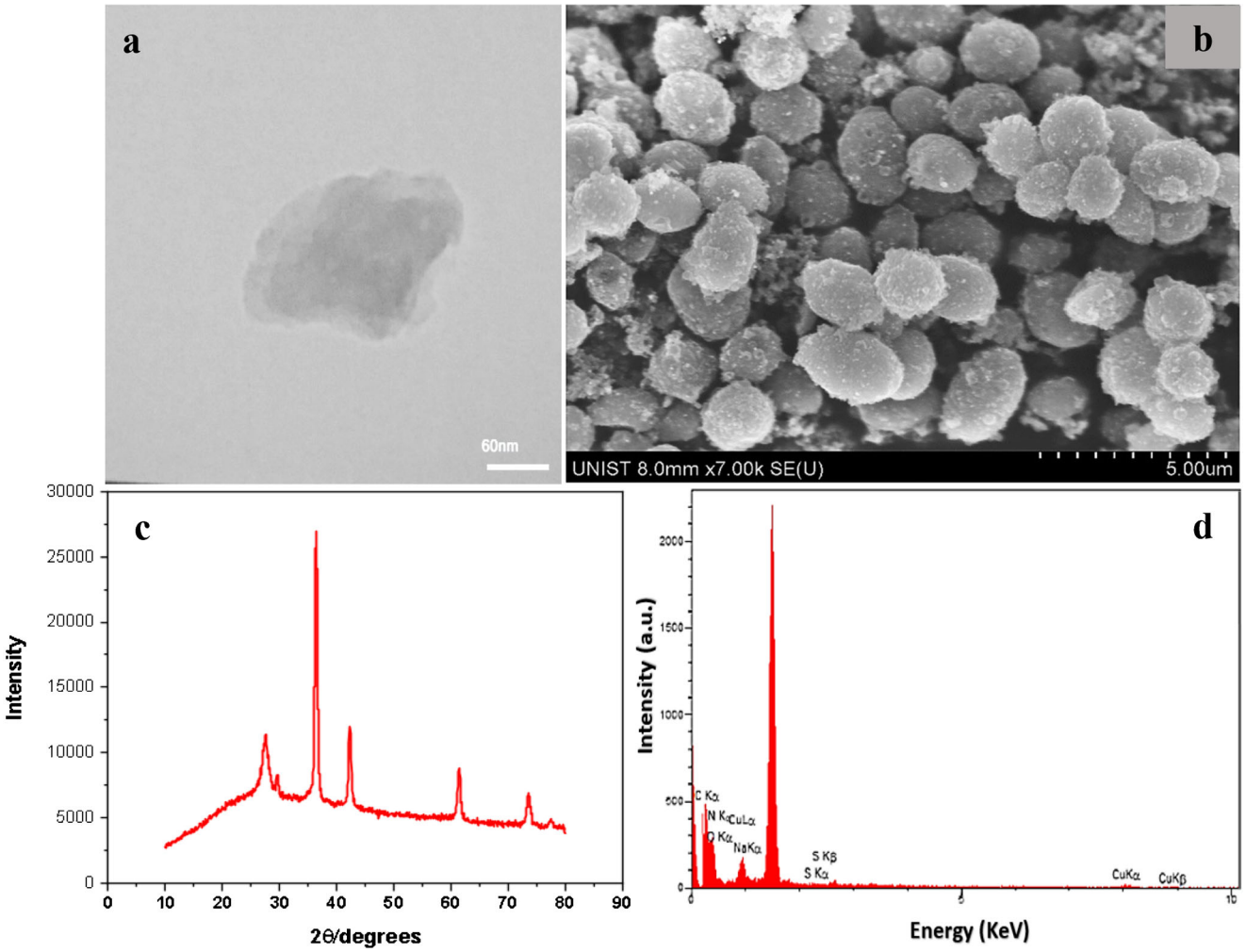

Fig. 1 (a) TEM image of g-C_3N_4 nanosheets, (b) SEM image of g-C_3N_4@Cu_2O composites, (c) XRD pattern of g-C_3N_4@Cu_2O composites, and (d) EDX analysis of g-C_3N_4@Cu_2O composites

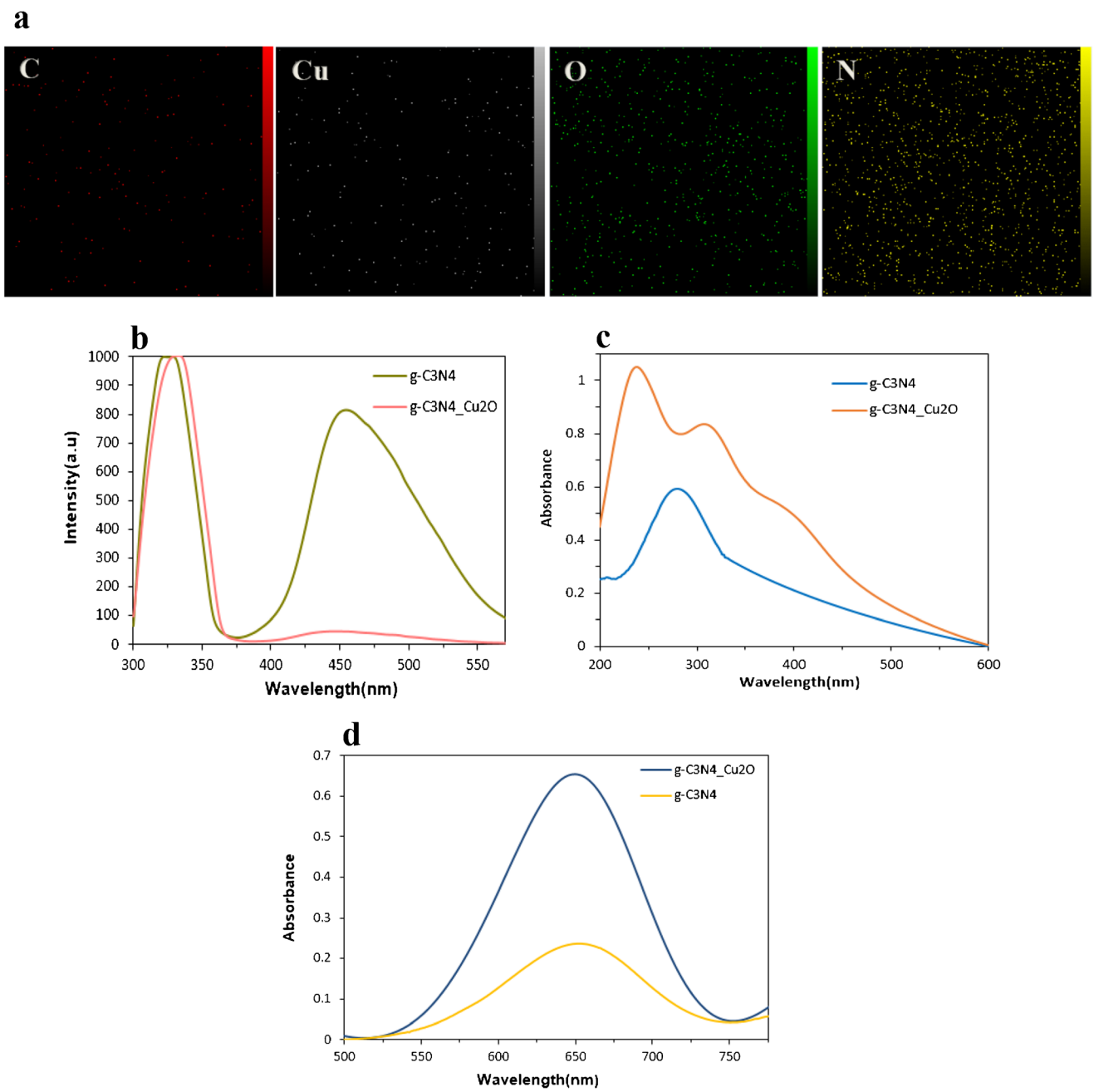

Fig. 2 (a) EDX mapping analysis, (b) fluorescence spectra (at excitation wavelength of 320 nm); high fluorescence emission of g-C_3N_4 was reduced by nearly 94% in g-C_3N_4@Cu_2O, (c) UV-Vis spectra of g-C_3N_4 and g-C_3N_4@Cu_2O (indicating the changes in number, intensity, and location of absorption peak), and (d) comparison the peroxidase-like activity of g-C_3N_4 and g-C_3N_4@Cu_2O following the addition of TMB and H_2O_2; the peroxidase-like activity was efficiently increased in g-C_3N_4@Cu_2O

27.6° indicated the existence of g-C_3N_4 nanosheet in the composite, while the other diffraction peaks at 2θ = 29.6°, 36.5°, 42.4°, 61.5°, and 73.7° were matched well with the standard pattern of Cu_2O, corresponding to (110), (111), (200), (220), and (311) planes of Cu_2O, respectively. According to Fig. 1d, EDX analysis proved the presence of used elements such as copper (Cu), oxygen (O), carbon (C), and nitrogen (N) in the synthesized g-C_3N_4@Cu_2O. EDX mapping analysis also confirmed previous data by providing the frequency distribution of elements in g-C_3N_4@Cu_2O (Fig. 2a). Fluorescence spectroscopy analysis confirmed the high fluorescence of g-C_3N_4 nanosheets, as one of their considerable properties. As shown in Fig. 2b, the intensity of fluorescence emission was reduced by nearly 94% in g-C_3N_4@Cu_2O compared with single g-C_3N_4 nanosheets.. Moreover, as shown in Fig. 2c, the observed variations in the UV-Vis spectra of g-C_3N_4 nanosheets and g-C_3N_4@Cu_2O composite (including

differences in number, intensity, and location of absorption peak) provided further evidence of the composite formation. In addition, the peroxidase-like activity of the structures was also studied by adding equal amounts of TMB and H_2O_2, and measurement of absorption spectra. As shown in Fig. 2d, comparison of absorption spectra indicated a significant increase in peroxidase-like activity after the formation of g-C_3N_4@Cu_2O composites.

Evaluating the interaction of aptamer with g-C_3N_4@Cu_2O

In order to investigate the interaction between the aptamer and g-C_3N_4@Cu_2O composite, the absorption spectra of the g-C_3N_4@Cu_2O containing aptamers were compared with absorption spectra of the g-C_3N_4@Cu_2O without aptamer. The interaction of aptamer with g-C_3N_4@Cu_2O was concluded from the objective changes shown in Fig. S1A. According to dynamic light scattering (DLS) measurements, the zeta potential values of the g-C_3N_4@Cu_2O containing aptamers and the one without aptamer were determined for examination of surface electric charge changes. Zeta potential of the sample without aptamer was −11, while this value for the sample with aptamers was −39. These results showed that the surface charge of the composite was negative by itself, but this value became more negative after the interaction with aptamers. The UV-Vis spectra, which was obtained after adding TMB and H_2O_2, indicated that the involvement of composite by aptamers led to an obvious decrease in peroxidase-like activity (Fig. S1B) and the color changes verified this decline clearly (Fig. S1C).

Optimization of effective parameters

As a colorimetric method, optimization of TMB and H_2O_2 concentrations was obligatory to achieve the highest detection performance. First, the effect of different concentrations of TMB (10 μL, 5-8-10-12 and 15 mM) was studied in presence of a constant value of H_2O_2 (10 μL, 1 M). According to Fig. S2A, optimum concentration of TMB was obtained 12 mM, which caused the maximum increase in catalytic activity maintaining the absorption range less than 1. The same process was done to optimize H_2O_2 concentration while the concentration of 12 mM TMB was fixed. Similarly, among H_2O_2 concentrations (10 μL, 0.5-1-2-3 and 4 M), 3 M was chosen as the optimum (Fig. S2B). The optimization of aptamer concentration would increase the quenching rate of catalytic activity of g-C_3N_4@Cu_2O. Among the different studied concentrations of aptamer (60 μL, 2-2.5-3-5-7and 10 μM), 5 μM was selected for the quench of catalytic activity, considering the slight difference between the results of 5 μM and 7 μM (Fig. S2C). Incubation time of bacteria was another necessary parameter to optimize. As shown in Fig. S2D, the best incubation time of *S. typhimurium* for this aptasensor was obtained between 1.5 and 2 h.

Principles of *S. typhimurium* detection

After ensuring the interaction of aptamers with g-C_3N_4@Cu_2O, a certain concentration of *S. typhimurium* was added to the prepared aptasensor, and the changes in peroxidase-like activity were monitored after the addition of TMB and H_2O_2. According to Fig. S3, following the addition of *S. typhimurium* to aptasensor solution, the catalytic activity was increased, while this occurrence was not observed in none of the controls. This process demonstrated that aptamers have joined *S. typhimurium* specifically, and as a result, their interaction with g-C_3N_4@Cu_2O was enfeebled. Consequently, the peroxidase-like activity of g-C_3N_4@Cu_2O was strengthened.

Sensitivity of aptasensor

In order to quantitative detection of *S. typhimurium*, there was need to know the bacterial concentrations of serial dilution by several repetitions of the plate count method as standard method. Then, certain concentrations of *S. typhimurium* from 1.5 to 1.5×10^5 were added to the constant value of aptasensor solution separately, and the absorbance of each one was examined following the addition of TMB and H_2O_2. As a result, the new method was able to provide a range of blue colors correlated with the concentration of *S. typhimurium* (Fig. 3a), which could be interpreted to quantitative amounts by UV-Vis spectrometer. As presented in Fig. 3b, a standard calibration curve was achieved with a linear range from 1.5×10^1 to 1.5×10^5 CFU/ml in which the absorbance increases with increasing the concentration of *S. typhimurium*. The regression equation was written as $Y = 0.0588X + 0.2347$, where Y is the absorbance and X is the concentration of *S. typhimurium*. The correlation coefficient was calculated to be 0.9768. Furthermore, the detection limit of 15 CFU/ml was calculated according to the formula: 3STD/m (where STD is the standard deviation of the prepared aptasensor without target and m is the slope of the calibration curve [18]).

The diagnostic ability of the introduced aptasensor in comparison with previous aptasensors for *S. typhimurium* is summarized in Table 1. In addition to the simplicity of usage, cost-effectiveness, rapidity of operation, and the capability of portable analysis, this new diagnostic system demonstrated high potential for

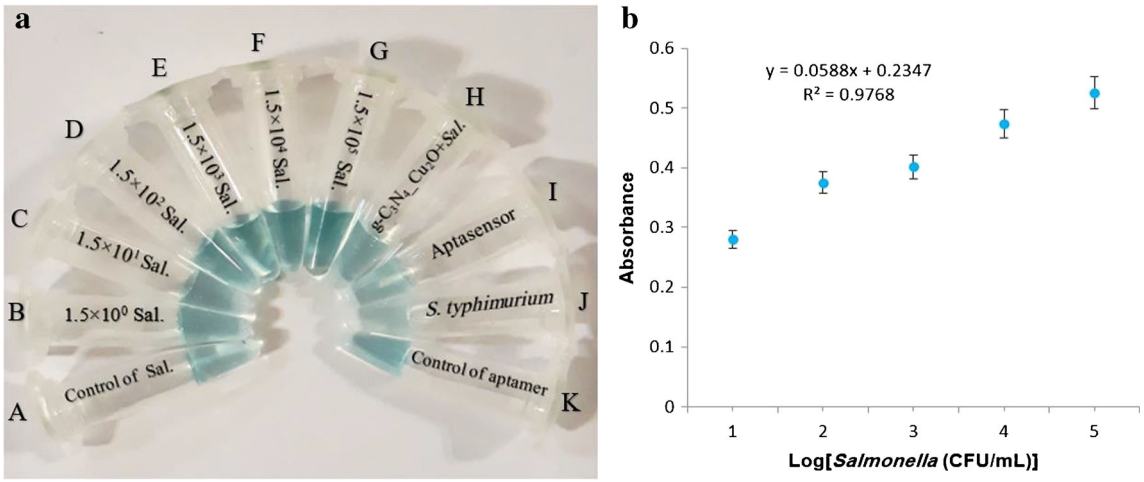

Fig. 3 (a) Positive correlation between the intensity of blue color and the concentration of *S. typhimurium* (A: Control of *S. typhimurium* (aptasensor + sterile water), B_G: Aptasensor + different concentrations of *S. typhimurium*, H: G-C_3N_4@Cu_2O + *S. typhimurium*, I: Aptasensor (g-C_3N_4@Cu_2O/aptamer), J: *S. typhimurium* (first source of serial dilution), K: Control of aptamer. (b) The calibration curve illustrating the positive correlation between the absorbance and the logarithm of different concentration of *S. typhimurium* within the range of 1.5×10^1 to 1.5×10^5 CFU/ml

sensitive, selective, and reliable whole cell detection of *S. typhimurium*.

Operation assessment of paper-based model of aptasensor

To evaluate the paper-based model of aptasensor, different concentrations of *S. typhimurium* were added to the paper-chips containing aptasensor solution. As illustrated in Fig. 4a, in presence of *S. typhimurium*, the color of papers was changed to blue after adding TMB and H_2O_2. Due to the pores within the paper-chip, which increase the rate of interactions between the aptamer and bacteria, the paper-based model of aptasensor was not dependent on incubation time. Accordingly, the portable model of this method could identify *S. typhimurium* in just 6 min by providing the visible results to the naked eye.

Evaluation of selectivity

To investigate the selectivity of this aptasensor toward *S. typhimurium*, the aptasensor was examined by other pathogens including *Escherichia coli*, *Staphylococcus aureus*, and *Pseudomonas aeruginosa* in the same conditions. The results showed that none of these strains could cause the similar color and absorbance with *S. typhimurium* after exposure to the aptasensor (Fig. 4b). The selectivity of an aptasensor refers to the specificity of applied aptamer toward the target. The used aptamer was specifically designed for *S. typhimurium* outer membrane proteins (OMPs) [29]. Thus, it does not tend to attach the other bacteria, considering the existence of different proteins on other cell membranes.

S. typhimurium detection in milk

The diagnostic potency of aptasensor was evaluated in milk as the real sample. Thus, the aptasensor was applied to evaluate

Table 1 Comparison of recently reported aptasensors for *S. typhimurium* detection

Nanomaterial(s)	Method(s)	Linear range (CFU/ml)	LOD (CFU/ml)	Reference
Gold nanoparticles (AuNP)	Colorimetric	3.3×10^1 to 3.3×10^6	33	[32]
Gold nanoparticles (AuNP)	Localized surface plasmon resonance (LSPR) sensing	12 to 5×10^5	10^4	[33]
Magnetic nanoparticles (MNPs)	Immunomagnetic separation, enzymatic catalysis, and electrical signal-of	3.7×10^1 to 3.7×10^6	33	[34]
Spiny gold nanoparticles (SGNPs)	Surface-enhanced Raman spectroscopy (SERS)	10^1 to 10^5	4	[19]
Pt@ZIF-8 nanocatalysts	Colorimetric	10^1 to 10^4	11	[35]
G-C_3N_4@Cu_2O composite	Colorimetric	1.5×10^1 to 1.5×10^5	15	This work

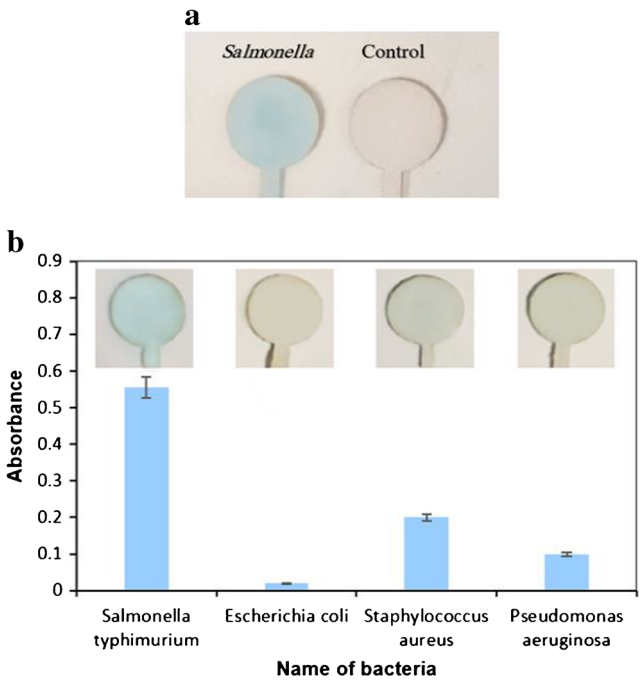

Fig. 4 (a) Paper-based detection of *S. typhimurium*; observation of blue color on the paper-chip after adding the sample as well as TMB and H_2O_2 indicates the presence of *S. typhimurium* in the tested sample. (b) Selective detection of *S. typhimurium*; the obtained results of this method for *E. coli* and *S. aureus* (as two of common foodborne pathogens) as well as *P. aeruginosa* (as an environmental pathogen) could confirm the selectivity of aptasensor toward *S. typhimurium*

S. typhimurium existence in the spiked milk sample. The response values, shown in Table S1, could indicate a favorable coordination with the calibration curve. For each sample, the concentration of *S. typymurium* was measured by the plate count method as a popular standard method for counting bacteria in microbiology. The results obtained from the introduced aptasensor and the standard method were satisfactorily analogous. As brought in Table S1, the percent recovery was defined in the range of 96 to 104%, which affirmed the appropriate accuracy of this method for detection of *S. typhimurium* in milk or other food samples (Fig. S4).

Conclusion

In conclusion, a novel composite of g-C_3N_4 nanosheets and Cu_2O nanocrystals was synthesized through this study, which represented a collection of significant properties for designing new diagnostic systems. The simultaneous ability of this composite to provide the catalytic activity and the interaction with aptamer made it efficiently appropriate for aptasensors. Hence, a novel aptasensor based on g-C_3N_4@Cu_2O was fabricated which could successfully detect very low concentrations of *S. typhimurium* as one of the most important foodborne pathogens. Despite the reliable diagnostic function, this colorimetric method could provide visually accurate results, which were visible with naked eye. This sensitive, rapid, affordable diagnostic system with the detection limit of 15 CFU/ml can be a hopeful approach for eliminating the persistent burden of *S. typhimurium* to public health and preventing the dangerous outbreaks of this pathogen in future.

Supplementary Information The online version contains supplementary material available at https://doi.org/10.1007/s00604-021-04745-w.

Funding The authors are grateful to the Research Council of University of Tehran for the financial support of this work.

Compliance with ethical standards

Conflict of interest The authors declare no competing interests.

References

1. Holban AM, Grumezescu AM (2018) Microbial contamination and food degradation, eds. Academic Press, London, United Kingdom
2. Crump JA, Sjölund-Karlsson M, Gordon MA, Parry CM (2015) Epidemiology, clinical presentation, laboratory diagnosis, antimicrobial resistance, and antimicrobial management of invasive Salmonella infections. Clin Microbiol Rev 28:901–937. https://doi.org/10.1128/CMR.00002-15
3. Torpdahl M, Lauderdale T-L, Liang S-Y, Li I, Wei S-H, Chiou C-S (2013) Human isolates of Salmonella enterica serovar Typhimurium from Taiwan displayed significantly higher levels of antimicrobial resistance than those from Denmark. Int J Food Microbiol 161:69–75. https://doi.org/10.1016/j.ijfoodmicro.2012.11.022
4. Inbaraj BS, Chen BH (2016) Nanomaterial-based sensors for detection of foodborne bacterial pathogens and toxins as well as pork adulteration in meat products. J Food Drug Anal 24:15–28. https://doi.org/10.1016/j.jfda.2015.05.001
5. Guadarrama C, Villaseñor T, Calva E (2014) The subtleties and contrasts of the LeuO regulator in Salmonella Typhi: implications in the immune response. Front Immunol 5:581. https://doi.org/10.3389/fimmu.2014.00581
6. Pashazadeh P, Mokhtarzadeh A, Hasanzadeh M, Hejazi M, Hashemi M, de la Guardia M (2017) Nano-materials for use in sensing of salmonella infections: recent advances. Biosens Bioelectron 87:1050–1064. https://doi.org/10.1016/j.bios.2016.08.012
7. Srisa-Art M, Boehle KE, Geiss BJ, Henry CS (2018) Highly sensitive detection of Salmonella typhimurium using a colorimetric paper-based analytical device coupled with immunomagnetic separation. Anal Chem 90:1035–1043. https://doi.org/10.1021/acs.analchem.7b04628
8. Reta N, Saint CP, Michelmore A, Prieto-Simon B, Voelcker NH (2018) Nanostructured electrochemical biosensors for label-free detection of water-and food-borne pathogens. ACS Appl Mater Interfaces 10:6055–6072. https://doi.org/10.1021/acsami.7b13943
9. Ranjbar S, Shahrokhian S, Nurmohammadi F (2018) Nanoporous gold as a suitable substrate for preparation of a new sensitive

electrochemical aptasensor for detection of Salmonella typhimurium. Sensors Actuators B Chem 255:1536–1544. https://doi.org/10.1016/j.snb.2017.08.160
10. Shahsavar K, Hosseini M, Shokri E, Ganjali MR, Ju H (2017) A sensitive colorimetric aptasensor with a triple-helix molecular switch based on peroxidase-like activity of a DNAzyme for ATP detection. Anal Methods 9:4726–4731. https://doi.org/10.1039/C7AY01381G
11. Kermani HA, Hosseini M, Miti A, Dadmehr M, Zuccheri G, Hosseinkhani S, Ganjali MR (2018) A colorimetric assay of DNA methyltransferase activity based on peroxidase mimicking of DNA template Ag/Pt bimetallic nanoclusters. Anal Bioanal Chem 410:4943–4952. https://doi.org/10.1007/s00216-018-1143-2
12. Dehghani Z, Hosseini M, Mohammadnejad J, Bakhshi B, Rezayan AH (2018) Colorimetric aptasensor for Campylobacter jejuni cells by exploiting the peroxidase like activity of Au@ Pd nanoparticles. Microchim Acta 185:448. https://doi.org/10.1007/s00604-018-2976-2
13. Dehghani Z, Hosseini M, Mohammadnejad J, Ganjali MR (2019) New colorimetric DNA sensor for detection of Campylobacter jejuni in Milk sample based on peroxidase-like activity of gold/platinium nanocluster. ChemistrySelect 4:11687–11692. https://doi.org/10.1002/slct.201901815
14. Abarghoei S, Fakhri N, Borghei YS, Hosseini M, Ganjali MR (2019) A colorimetric paper sensor for citrate as biomarker for early stage detection of prostate cancer based on peroxidase-like activity of cysteine-capped gold nanoclusters. Spectrochim Acta A Mol Biomol Spectrosc 210:251–259. https://doi.org/10.1016/j.saa.2018.11.026
15. Hosseini M, Aghazadeh M, Ganjali MR (2017) A facile one-pot synthesis of cobalt-doped magnetite/graphene nanocomposite as peroxidase mimetics in dopamine detection. New J Chem 41:12678–12684. https://doi.org/10.1039/C7NJ02082A
16. Naderi M, Hosseini M, Ganjali MR (2018) Naked-eye detection of potassium ions in a novel gold nanoparticle aggregation-based aptasensor. Spectrochim Acta A Mol Biomol Spectrosc 195:75–83. https://doi.org/10.1016/j.saa.2018.01.051
17. Xu H-H, Deng H-H, Lin X-Q, Wu Y-Y, Lin X-L, Peng H-P, Liu A-L, Xia X-H, Chen W (2017) Colorimetric glutathione assay based on the peroxidase-like activity of a nanocomposite consisting of platinum nanoparticles and graphene oxide. Microchim Acta 184:3945–3951. https://doi.org/10.1007/s00604-017-2429-3
18. Chinnappan R, AlAmer S, Eissa S, Rahamn AA, Salah KMA, Zourob M (2018) Fluorometric graphene oxide-based detection of Salmonella enteritis using a truncated DNA aptamer. Microchim Acta 185:61. https://doi.org/10.1007/s00604-017-2601-9
19. Xu X, Ma X, Wang H, Wang Z (2018) Aptamer based SERS detection of Salmonella typhimurium using DNA-assembled gold nanodimers. Microchim Acta 185:7–325
20. Lee J, Jung J, Lee CS, Ha TH (2017) Design and optimization of an ultra-sensitive hairpin DNA aptasensor for Salmonella detection. RSC Adv 7:34933–34938. https://doi.org/10.1039/C7RA06000A
21. Mesgari F, Beigi SM, Salehnia F, Hosseini M, Ganjali MR (2019) Enhanced electrochemiluminescence of Ru (bpy) 32+ by Sm2O3 nanoparticles decorated graphitic carbon nitride nano-sheets for pyridoxine analysis. Inorg Chem Commun 106:240–247. https://doi.org/10.1016/j.inoche.2019.05.023
22. Salehnia F, Hosseini M, Ganjali MR (2017) A fluorometric aptamer based assay for cytochrome C using fluorescent graphitic carbon nitride nanosheets. Microchim Acta 184:2157–2163. https://doi.org/10.1007/s00604-017-2130-6
23. Nemati F, Zare-Dorabei R (2019) A ratiometric probe based on Ag2S quantum dots and graphitic carbon nitride nanosheets for the fluorescent detection of cerium. Talanta 200:249–255. https://doi.org/10.1016/j.talanta.2019.03.059
24. Fakhri N, Salehnia F, Beigi SM, Aghabalazadeh S, Hosseini M, Ganjali MR (2019) Enhanced peroxidase-like activity of platinum nanoparticles decorated on nickel-and nitrogen-doped graphene nanotubes: colorimetric detection of glucose. Microchim Acta 186:385. https://doi.org/10.1007/s00604-019-3489-3
25. Feng T, Chen X, Qiao X, Sun Z, Wang H, Qi Y, Hong C (2016) Graphene oxide supported rhombic dodecahedral Cu2O nanocrystals for the detection of carcinoembryonic antigen. Anal Biochem 494:101–107. https://doi.org/10.1016/j.ab.2015.11.004
26. Fakhri N, Hosseini M, Tavakoli O (2018) Aptamer-based colorimetric determination of Pb 2+ using a paper-based microfluidic platform. Anal Methods 10:4438–4444. https://doi.org/10.1039/C8AY01331D
27. Teengam P, Siangproh W, Tuantranont A, Vilaivan T, Chailapakul O, Henry CS (2017) Multiplex paper-based colorimetric DNA sensor using pyrrolidinyl peptide nucleic acid-induced AgNPs aggregation for detecting MERS-CoV, MTB, and HPV oligonucleotides. Anal Chem 89:5428–5435. https://doi.org/10.1021/acs.analchem.7b00255
28. Odumeru JA, León-Velarde CG (2012) Salmonella detection methods for food and food ingredients. Salmonella-a dangerous foodborne pathogen. Rijeka, Croatia. InTec:373–392. https://doi.org/10.5772/29526
29. Joshi R, Janagama H, Dwivedi HP, Kumar TMAS, Jaykus L-A, Schefers J, Sreevatsan S (2009) Selection, characterization, and application of DNA aptamers for the capture and detection of Salmonella enterica serovars. Mol Cell Probes 23:20–28. https://doi.org/10.1016/j.mcp.2008.10.006
30. Hosseini M (2020) Fast and selective whole cell detection of Staphylococcus aureus bacteria in food samples by paper based colorimetric nanobiosensor using peroxidase-like catalytic activity of DNA-au/Pt bimetallic nanoclusters. Microchem J:105475. https://doi.org/10.1016/j.microc.2020.105475
31. Kuo M-Y, Hsiao C-F, Chiu Y-H, Lai T-H, Fang M-J, Wu J-Y, Chen J-W, Wu C-L, Wei K-H, Lin H-C (2019) Au@ Cu2O core@shell nanocrystals as dual-functional catalysts for sustainable environmental applications. Appl Catal B Environ 242:499–506. https://doi.org/10.1016/j.apcatb.2018.09.075
32. Chen S, Yang X, Fu S, Qin X, Yang T, Man C, Jiang Y (2020) A novel AuNPs colorimetric sensor for sensitively detecting viable Salmonella typhimurium based on dual aptamers. Food Control: 107281. https://doi.org/10.1016/j.foodcont.2020.107281
33. Oh SY, Heo NS, Shukla S, Cho H-J, Vilian ATE, Kim J, Lee SY, Han Y-K, Yoo SM, Huh YS (2017) Development of gold nanoparticle-aptamer-based LSPR sensing chips for the rapid detection of Salmonella typhimurium in pork meat. Sci Rep 7:1–10. https://doi.org/10.1038/s41598-017-10188-2
34. Hou Y, Cai G, Zheng L, Lin J (2019) A microfluidic signal-off biosensor for rapid and sensitive detection of Salmonella using magnetic separation and enzymatic catalysis. Food Control 103:186–193. https://doi.org/10.1016/j.foodcont.2019.04.008
35. Wang L, Huo X, Zheng L, Cai G, Wang Y, Liu N, Wang M, Lin J (2020) An ultrasensitive biosensor for colorimetric detection of Salmonella in large-volume sample using magnetic grid separation and platinum loaded zeolitic imidazolate Framework-8 nanocatalysts. Biosens Bioelectron 150:111862. https://doi.org/10.1016/j.bios.2019.111862